Nonlinear Domain Decomposition and Multilevel methods for solving Phase-Field Fracture Problems

Alena Kopaničáková, Hardik Kothari, Patrick Zulian, Rolf Krause

Euler Institute, Università della Svizzera italiana, Switzerland

CANUM 2020
June 14, 2022
Évian-les-Bains, France

Fracture problem

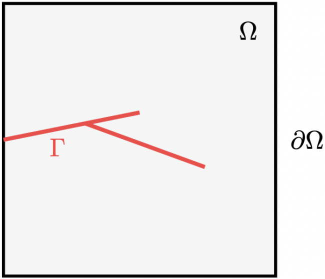

- When/where a crack propagates? How much it propagates and in which direction?

- Ad-hoc criterium needed, e.g.
  - maximum stress criteria [Erdogan and Sih, '63]
  - minimum strain energy density criteria [Sih, '73]
  - maximum energy release rate criteria [Wu, '78]
  - critical stress or strain criteria [Ainsworth, '03]

- Computationally challenging due to discontinuities in the displacement field

- Discontinuities can be resolved at the element boundaries by
  - duplicating nodes [Moës et al., '99]
  - remeshing [Bouchard et al., '03]

Variational approach to fracture

Total potential energy: [Ambrosio, Tortorelli '90]

$$\tilde{\mathcal{E}}(\boldsymbol{u}, \Gamma) = \underbrace{\int_{\Omega \setminus \Gamma} \psi_e(\boldsymbol{u}) \, d\Omega}_{\text{elastic energy}} + \underbrace{\int_{\Gamma} \mathcal{G}_c \, d\Gamma}_{\text{fracture energy}}$$

- $\mathcal{G}_c$, critical energy release rate
- amount of strain energy required for the crack propagation

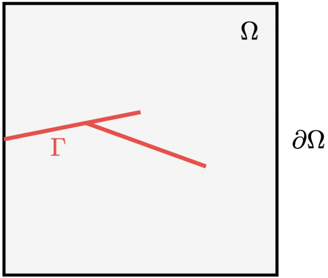

Regularization of fracture energy

[Bourdin, Francfort, Marigo, '00, '07, '08]

$$\int_{\Gamma} \mathcal{G}_c \; d\Gamma \approx \underbrace{\int_{\Omega} \frac{\mathcal{G}_c}{2 l_s} \; c^2 \; d\Omega}_{\text{reaction term}} + \underbrace{\int_{\Omega} \frac{G_c l_s}{2} \; |\nabla c|^2 \; d\Omega}_{\text{diffusion term}}.$$

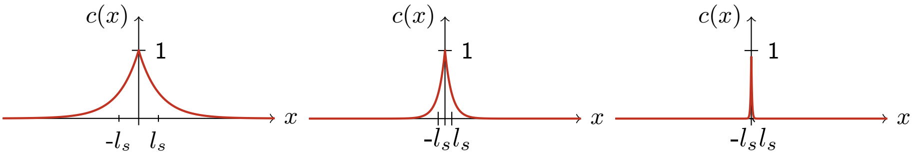

Length-scale parameter l_s:

- Controls the thickness of the damaged region
- Γ convergence [Braides, '98]: $l_s \to 0$ gives rise to a sharp crack surface Γ
- Value of l_s tied to the refinement as $l_s > h$ has to be fulfilled [Miehe et al., '10]

Phase-field variational form

Total potential energy: [Ambrosio, Tortorelli '90]

$$\tilde{\mathcal{E}}(\boldsymbol{u}, \Gamma) = \underbrace{\int_{\Omega \setminus \Gamma} \psi_e(\boldsymbol{u}) \, d\Omega}_{\text{elastic energy}} + \underbrace{\int_{\Gamma} \mathcal{G}_c \, d\Gamma}_{\text{fracture energy}}$$

Regularized total potential energy: [Bourdin et al., '00; Miehe et al., '10]

$$\mathcal{E}(\boldsymbol{u}, c) = \underbrace{\int_{\Omega} (1-c)^2 \psi_e^+(\boldsymbol{u}) + \psi_e^-(\boldsymbol{u}) \, d\Omega}_{\text{elastic energy}} + \underbrace{\int_{\Omega} \mathcal{G}_c \left(\frac{1}{2 l_s} c^2 + \frac{l_s}{2} \mid \nabla c \mid^2 \right) d\Omega}_{\text{volumetric approximation of fracture energy}}$$

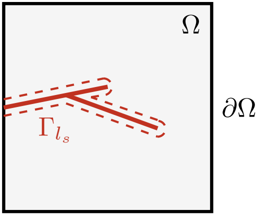

Phase field approach:

- The fracture problem is transformed into a continuous problem
- The crack is modelled in a diffused manner
- Transition represented by the phase field parameter, $c \in [0, 1]$

Minimization problem

- At each pseudo-time step

$$(\mathbf{u}^t, c^t) = \underset{\substack{\mathbf{u}=\mathbf{u}_D^t \text{ on } \partial\Omega_D \\ \partial_t c \geqslant 0}}{\arg\min} \; \mathcal{E}(\mathbf{u}, c)$$

- Penalty approach to enforce irreversibility condition

$$(\mathbf{u}^t, c^t) = \underset{\mathbf{u}=\mathbf{u}_D^t \text{ on } \partial\Omega_D}{\arg\min} \; \Psi(\mathbf{u}, c) := \mathcal{E}(\mathbf{u}, c) + \frac{\gamma}{2} \int_\Omega (\langle c - c^{t-1} \rangle_-)^2 \, d\Omega,$$

$$\text{where, } \langle x \rangle_- := \begin{cases} x & \text{if } x < 0 \\ 0 & \text{otherwise} \end{cases}$$

- Constrained optimization approach to enforce irreversibility condition

$$(\mathbf{u}^t, c^t) = \underset{\mathbf{u}=\mathbf{u}_D^t \text{ on } \partial\Omega_D}{\arg\min} \; \mathcal{E}(\mathbf{u}, c)$$

$$\text{subject to } c \geqslant c^{t-1}$$

Nonlinear system of equations

- Variational form: Find a pair $(\mathbf{u}, c) \in \boldsymbol{\mathcal{V}}^t \times H^1(\Omega)$, such that

$$\nabla_{\mathbf{u}} \Psi(\mathbf{u}, c; \mathbf{v}) = 0, \quad \forall \mathbf{v} \in \boldsymbol{\mathcal{V}}_0$$
$$\nabla_c \Psi(\mathbf{u}, c; w) = 0, \quad \forall w \in H^1(\Omega),$$

where, $\boldsymbol{\mathcal{V}}^t := \{\boldsymbol{u} \in \boldsymbol{H}^1(\Omega) | \boldsymbol{u} = \boldsymbol{g}^t \text{ on } \partial\Omega_D\}$,
$\boldsymbol{\mathcal{V}}^0 := \{\boldsymbol{u} \in \boldsymbol{H}^1(\Omega) | \boldsymbol{u} = 0 \text{ on } \partial\Omega_D\}$

- Algebraic coupled problem: Find $(\mathbf{u}^*, c^*) \in \mathbb{R}^{nd} \times \mathbb{R}^n$ such that

$$F(\mathbf{u}^*, c^*) = \begin{bmatrix} F_u(\mathbf{u}^*, c^*) \\ F_c(\mathbf{u}^*, c^*) \end{bmatrix} = \mathbf{0}$$

- Coupled problem is non-convex
- Slow convergence due to unbalanced and highly localized nonlinearities
  - coupling between the displacement and the phase-field
  - locally varying material stiffness
  - steep gradients of the phase-field function

Nonlinear preconditioning[Cai, Keyes '02; Dolean et al. '16]

Instead of solving $F(\mathbf{x}) = 0$, we solve

$$\mathcal{F}(\mathbf{x}) = G(\underbrace{F(\mathbf{x})}_{\mathbf{y}}) = 0$$

Properties of the preconditioner G :

- $G \approx F^{-1}$ in some sense
- $G(F(\mathbf{x}))$ should have more balanced nonlinearities
- If $G(\mathbf{y}) = 0$, then $\mathbf{y} = 0$, where $\mathbf{y} = F(\mathbf{x})$
- Solving $G(F(\mathbf{x})) = 0$ should be easier than solving $F(\mathbf{x}) = 0$

Schwarz Preconditioned IN method [Cai, Keyes '02; Liu, Keyes '15]

- Employ field-split approach, thus by decomposing $\mathbf{x}$ as $[\mathbf{u}, c]^T$, i.e.,

$$G(F(\mathbf{u}, c)) := \mathcal{F}(\mathbf{u}, c) := \begin{bmatrix} \mathcal{F}_u(\mathbf{u}, c) \\ \mathcal{F}_c(\mathbf{u}, c) \end{bmatrix} := \mathbf{0}$$

- Explicit knowledge of preconditioner G is typically not available
- Construct $\mathcal{F}$ implicitly using knowledge about F and $\mathbf{x}$

ASPIN: Find $\mathcal{F}_u$ such that $F_u(\mathbf{u} - \mathcal{F}_u, c) = 0$

Find $\mathcal{F}_c$ such that $F_c(\mathbf{u}, c - \mathcal{F}_c) = 0$

$$\implies \mathcal{F}_A(\mathbf{u}, c) = \begin{bmatrix} \mathcal{F}_u(\mathbf{u}, c) \\ \mathcal{F}_c(\mathbf{u}, c) \end{bmatrix}$$

MSPIN: Find $\mathcal{F}_u$ such that $F_u(\mathbf{u} - \mathcal{F}_u, c) = 0$

Find $\mathcal{F}_c$ such that $F_c(\mathbf{u} - \mathcal{F}_u, c - \mathcal{F}_c) = 0$

$$\implies \mathcal{F}_{\mathsf{M}}(\mathbf{u}, c) = \begin{bmatrix} \mathcal{F}_u(\mathbf{u}, c) \\ \mathcal{F}_c(\mathbf{u}, c) \end{bmatrix}$$

SPIN algorithm

1. For a given $\mathbf{u}^{(k)}, c^{(k)}$, perform local/decoupled step:

   ASPIN:
   Find $\mathbf{u}^*$ by solving $F_u(\mathbf{u}^*, c^{(k)})=0$
   Find c^* by solving $F_c(\mathbf{u}^{(k)}, c^*)=0$

   MSPIN:
   Find $\mathbf{u}^*$ by solving $F_u(\mathbf{u}^*, c^{(k)})=0$
   Find c^* by solving $F_c(\mathbf{u}^*, c^*)=0$

2. Evaluate preconditioned residual as $\mathcal{F}_{A/M}^{(k)} = \begin{bmatrix} \mathbf{u}^{(k)} - \mathbf{u}^* \\ c^{(k)} - c^* \end{bmatrix}$

3. Find $\mathbf{p}^{(k)}$ by solving $(\tilde{\mathcal{F}}'_{A/M})^{(k)}\mathbf{p}^{(k)} = -\mathcal{F}_{A/M}^{(k)}$ inexactly, such that

$$\|(\tilde{\mathcal{F}}'_{A/M})^{(k)}\mathbf{p}^{(k)} + \mathcal{F}_{A/M}^{(k)}\| \leq \eta \|\mathcal{F}_{A/M}^{(k)}\|$$

4. Find $\alpha^{(k)}$ using a backtracking algorithm

5. $\begin{bmatrix} \mathbf{u}^{(k+1)} \\ c^{(k+1)} \end{bmatrix} = \begin{bmatrix} \mathbf{u}^{(k)} \\ c^{(k)} \end{bmatrix} + \alpha^{(k)}\mathbf{p}^{(k)}$

Jacobian of the preconditioned residual system

- Jacobian ${\mathcal{F}_A}'$ can be written as follows:

$$\mathcal{F}_\mathsf{A}' = \begin{bmatrix} \frac{\partial F_u}{\partial \delta_u} & \\ & \frac{\partial F_c}{\partial \delta_c} \end{bmatrix}^{-1} \begin{bmatrix} \frac{\partial F_u}{\partial \delta_u} & \frac{\partial F_u}{\partial \mathbf{u}} \\ \frac{\partial F_c}{\partial \mathbf{u}} & \frac{\partial F_c}{\partial \delta_c} \end{bmatrix} \quad \text{where, } \delta_u = \mathbf{u} - \mathcal{F}_u, \delta_c = c - \mathcal{F}_c$$

- Due to continuity of $F(\mathbf{x})$, we know, as $\mathcal{F}_u \to 0$ and $\mathcal{F}_c \to 0$
  $\delta_u \to \mathbf{u}$ and $\delta_c \to c$
- Now, Jacobian ${\mathcal{F}_A}'$ can be approximated as:

$$\mathcal{F}_A' \approx \begin{bmatrix} \frac{\partial F_u}{\partial \mathbf{u}} & \\ & \frac{\partial F_c}{\partial c} \end{bmatrix}^{-1} \underbrace{\begin{bmatrix} \frac{\partial F_u}{\partial \mathbf{u}} & \frac{\partial F_u}{\partial c} \\ \frac{\partial F_c}{\partial \mathbf{u}} & \frac{\partial F_c}{\partial c} \end{bmatrix}}_{F'}$$

- Similar computation can be carried out for the multiplicative variant

Considered solution strategies

- AM-ND: Alternate minimization with exact Newton (direct linear solver)
- AM-NK: Alternate minimization with exact Newton (Krylov linear solver)
- AM-INK: Alternate minimization with inexact Newton (Krylov linear solver)
- ASPIN: Additive Schwarz preconditioned inexact Newton
- MSPIN: Multiplicative Schwarz preconditioned inexact Newton

Implementation details

FEM discretization:

- Finite element framework MOOSE[Permann et al. '20]

Implementation of solution strategies:

- Utopia[Zulian, Kopanicakova et al. '21] (`https://bitbucket.org/zulianp/utopia`)
- PETSc backend is used for linear algebra and linear solvers (Krylov/direct)

Tension test (brutal crack propagation)

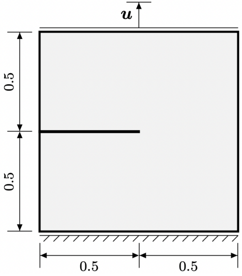

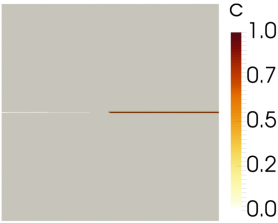

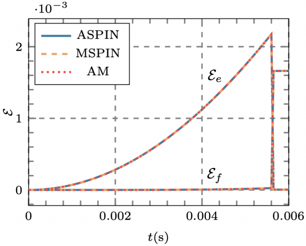

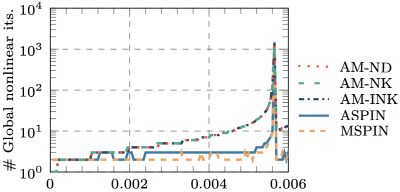

Solver	Time (min)	Speedup with respect to			
		AM-ND	AM-NK	AM-INK	ASPIN
AM-ND	243.21	–	–	–	–
AM-NK	131.61	1.85	–	–	–
AM-INK	129.64	1.88	1.02	–	–
ASPIN	126.64	1.92	1.04	1.02	–
MSPIN	115.34	2.11	1.14	1.12	1.10

Shear test (gradual crack propagation)

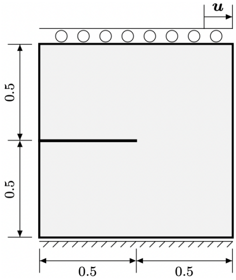

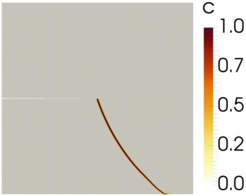

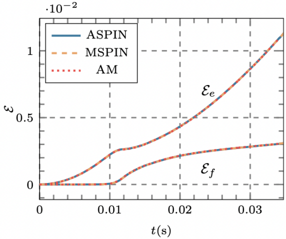

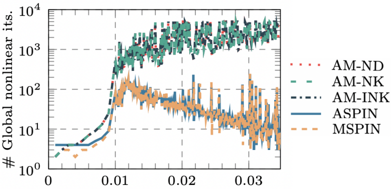

Solver	Time (min)	Speedup with respect to			
		AM-ND	AM-NK	AM-INK	ASPIN
AM-ND	5,792.72	–	–	–	–
AM-NK	3,886.39	1.49	–	–	–
AM-INK	3,476.33	1.66	1.12	–	–
ASPIN	118.56	48.86	32.78	29.32	–
MSPIN	115.23	50.27	33.72	30.17	1.03

L-shaped test (gradual crack propagation)

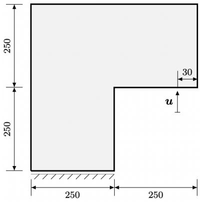

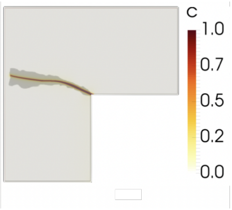

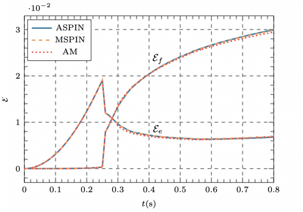

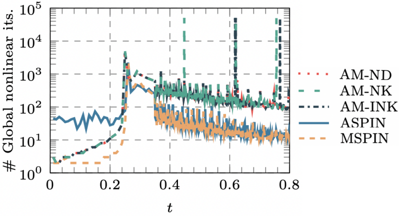

Solver	Time (min)	Speedup with respect to			
		AM-ND	AM-NK	AM-INK	ASPIN
AM-ND	4,353.61	–	–	–	–
AM-NK	4,492.19	0.96	–	–	–
AM-INK	3,590.13	1.21	1.25	–	–
ASPIN	556.03	7.83	8.08	6.45	–
MSPIN	469.90	9.26	9.56	7.64	1.18

Constrainted optimization approach

Find $(\boldsymbol{u}^t, c^t) \in \boldsymbol{\mathcal{V}}^t \times H^1(\Omega)$, such that

$$(\mathbf{u}^t, c^t) = \underset{\mathbf{u}=\mathbf{u}_D^t \text{ on } \partial\Omega_D}{\text{arg}\min} \Psi(\mathbf{u}, c)$$

$$\text{subject to } c \geqslant c^{t-1}$$

where $\boldsymbol{\mathcal{V}}^t := \{\boldsymbol{u} \in \boldsymbol{H}^1(\Omega) \mid \mathbf{u} = \mathbf{u}_D^t \text{ on } \partial\Omega_D\}$

- The energy functional is non-convex
- Bound constrained minimization problem

Trust-region (TR)

$$\arg\min_{\mathbf{x}\in\mathbb{R}^n} f(\mathbf{x})$$

subject to $\boldsymbol{l} \le \boldsymbol{x}$

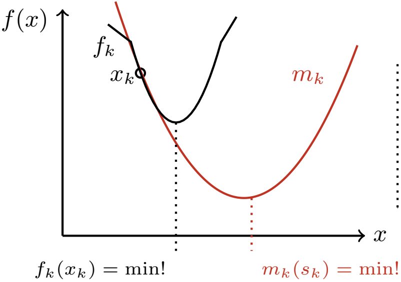

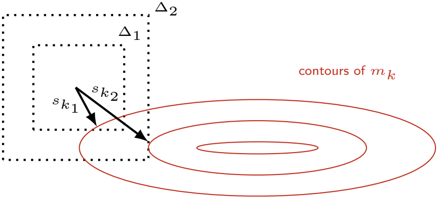

Trust-region algorithm

1. Generate the model problem $m_k(\mathbf{s}_k) = f_k + \langle g_k, \mathbf{s}_k \rangle + \frac{1}{2}\langle \mathbf{s}_k, H_k \mathbf{s}_k \rangle$
2. Solve TR subproblem

$$\begin{aligned} \text{arg} \min_{\mathbf{s}_k \in \mathbb{R}^n} & m_k(\mathbf{s}_k) \\ \text{subject to } & \|\mathbf{s}_k\|_\infty \leq \Delta_k \\ & \mathbf{s}_k \leq \boldsymbol{l} - \mathbf{x}_k \end{aligned}$$

3. Acceptance: $\rho = \frac{f(\mathbf{x}_k + \mathbf{s}_k) - f(\mathbf{x}_k)}{m(\mathbf{s}_k)} \geq \eta$ then: $\mathbf{x}_{k+1} = \mathbf{x}_k + \mathbf{s}_k$,
otherwise $\mathbf{x}_{k+1} = \mathbf{x}_k$, $\eta \in (0, 1)$
4. Update of the trust-region radius: Δ_k by means of ρ

Recursive multilevel trust-region method[1] (RMTR)

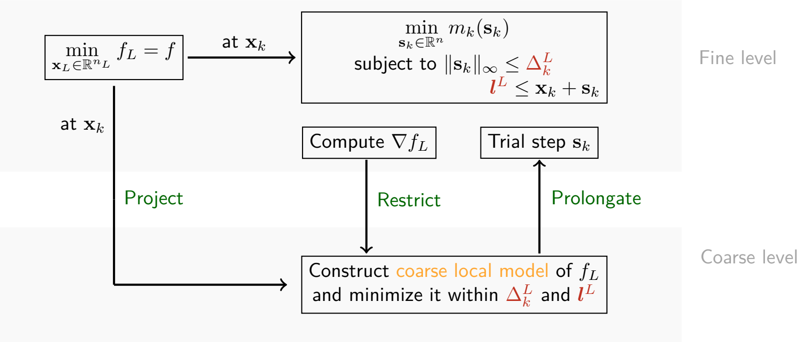

Ingredients:

1. Transfer operators
2. Level dependent objective functions
3. Multilevel treatment of constraints
4. Ensuring global convergence

[1] [Gratton et al., '06; Groß, Krause, '08]

1. Transfer Operators

- Prolongation operator $\mathbf{I}_l : \mathbb{R}^{n_{l-1}} \to \mathbb{R}^{n_l}$
  - transfers primal variables, such as correction $\mathbf{s}_k$
- Restriction operator $\mathbf{R}_l : \mathbb{R}^{n_l} \to \mathbb{R}^{n_{l-1}}$
  - transfers dual variables, such as gradient $\nabla f(\mathbf{x}_k)$

$$\mathbf{R}_l = (\mathbf{I}_l)^T$$

- Projection operator $\mathbf{P}_l : \mathbb{R}^{n_l} \to \mathbb{R}^{n_{l-1}}$
  - transfers primal variables, such as iterate $\mathbf{x}_k$

MOONoLith:[Krause, Zulian '16] `https://bitbucket.org/zulianp/par_moonolith`

2. Level-dependent objective functions [Brandt '77; Nash '00]

1st order consistency

$$h_{l-1}(\mathbf{x}_{l-1,0} + \mathbf{s}_{l-1}) := \underbrace{f_{l-1}(\mathbf{x}_{l-1,0} + \mathbf{s}_{l-1})}_{\text{coarse level model}} + \underbrace{\langle \delta\mathbf{g}, \mathbf{s}_{l-1} \rangle}_{\text{coupling term}}$$

where

$$\delta\mathbf{g} := \begin{cases} \mathbf{R}_l \nabla h_l(\mathbf{x}_{l,k}) - \nabla f_{l-1}(\mathbf{x}_{l-1,0}) & \text{if} \quad l < L \\ 0 & \text{if} \quad l = L \end{cases}$$

- Connects fine level objective function with the coarse level objective function
- First coarse-level correction goes in direction of the restricted fine level gradient
- Efficient, if coarse level model is good approximation to the fine level model

2. Level-dependent objective functions

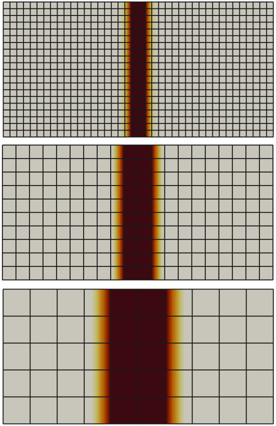

How to represent fracture?

- Fracture approximation width depends on the length-scale parameter l_s
- Length-scale parameter is tied to the refinement level as $l_s > h$ has to be fullfiled

2. Level-dependent objective functions

Solution dependent 2nd order consistency

$$h_{l-1}(\mathbf{x}_{l-1,0}+\mathbf{s}_{l-1}) := \underbrace{\tilde{f}_{l-1}(\mathbf{x}_{l-1,0}+\mathbf{s}_{l-1})}_{\text{modified coarse model}} + \underbrace{\langle \delta\mathbf{g}, \mathbf{s}_{l-1}\rangle + \chi_1(c,\epsilon)\frac{1}{2}\langle \mathbf{s}_{l-1}, \delta\boldsymbol{H}\mathbf{s}_{l-1}\rangle}_{\text{coupling terms}}$$

$$\tilde{f}_{l-1} := \tilde{\Psi}(\boldsymbol{u},c) := \int_\Omega \underbrace{\psi_e(\boldsymbol{u})}_{\text{elastic energy}} + \chi_2(c,\epsilon)\underbrace{\psi_f(c,l_s)}_{\text{fracture energy}} \, d\Omega$$

where

$$\delta\boldsymbol{H} := \begin{cases} \mathbf{R}_l\nabla^2 h_l(\mathbf{x}_{l,k})\mathbf{I}_l - \nabla^2 f_{l-1}(\mathbf{x}_{l-1,0}) & \text{if} \quad l < L, \\ 0 & \text{if} \quad l = L, \end{cases}$$

$$\chi_1(c,\epsilon) := \begin{cases} 1 & \text{if} \quad \max\limits_{i=0,\dots,n^L}(c_i) > \epsilon \\ 0 & \text{otherwise} \end{cases} \qquad \chi_2(c,\epsilon) := \begin{cases} 0 & \text{if} \quad \max\limits_{i=0,\dots,n^L}(c_i) > \epsilon \\ 1 & \text{otherwise} \end{cases}$$

3. Multilevel treatment of constraints

- Trust-region constraint on given level

$$\|\mathbf{s}_{l-1,k}\|_{\infty} \leq \Delta_{l-1,k}$$

- Trust-region constraint from finer level

$$\|\mathbf{I}_{l-1}\mathbf{s}_{l-1,*}\|_{\infty} \leq \Delta_{l}$$

- Irreversibility condition

$$(\mathbf{I}_{l-1}\mathbf{s}_{l-1,*})_i \leq (\boldsymbol{l}_l)_i$$

4. Ensuring convergence

- Pre-smoothing/Post-smoothing on each level:
  TR algorithm $\implies$ convergence of given level

- Coarse level correction does not exceed: fine level trust-region
  fine level constraints

- Measurement of the quality of the coarse level correction

$$\rho_{l,k} = \frac{h_l(\mathbf{x}_{l,k}) - h_l(\mathbf{x}_{l,k} + \mathbf{I}_{l-1}\mathbf{s}_{l-1})}{h_{l-1}(\mathbf{P}_l\mathbf{x}_{l,k}) - h_{l-1}(\mathbf{x}_{l-1,*})} = \frac{\text{fine level model decrease}}{\text{coarse level model decrease}}$$

- Acceptance only if $\rho_{l,k} \geq \eta$, otherwise correction is disposed

Benchmark: 3 fracture modes

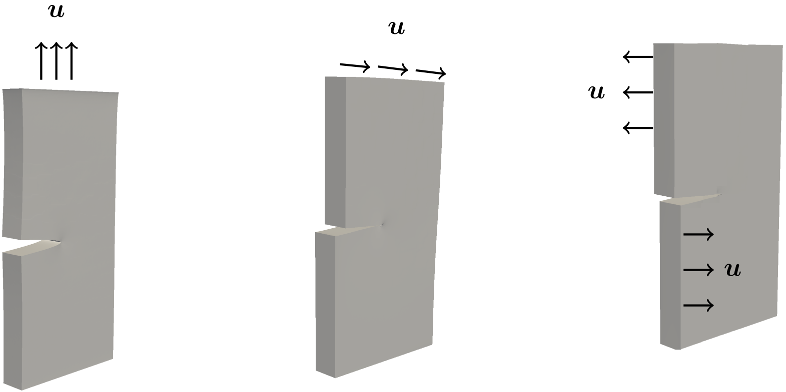

a) Tension b) Shear c) Tear

Benchmark: 3 fracture modes

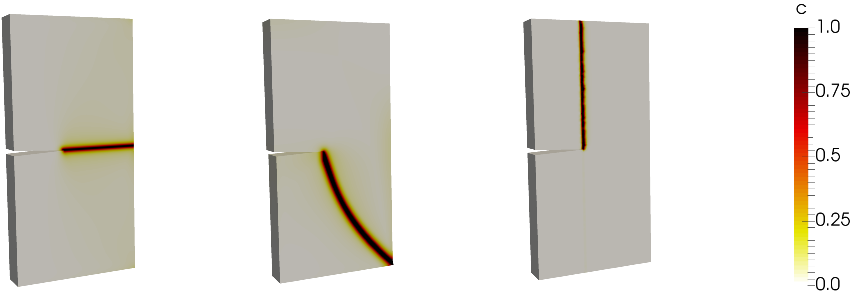

a) Tension b) Shear c) Tear

Effect of different coarse level models:

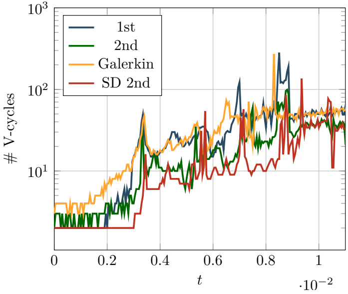

Number of nonlinear V-cycles over time-steps for shear test, specimen with $782,340$ dofs. RMTR was set up with 3 levels.

	Tension	Shear	Tear
1st order	1.17	2.79	3.15
2nd order	1.03	1.71	1.21
Galerkin	1.08	2.59	1.42

Speedup of RMTR method configured with the solution dependent 2nd order model with respect to alternative variants: 1st order consistency, 2nd order consistency and Galerkin model.

Number of nonlinear iterations over time

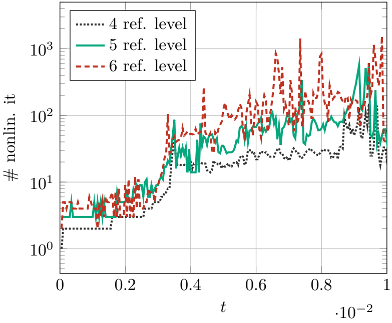

TR method

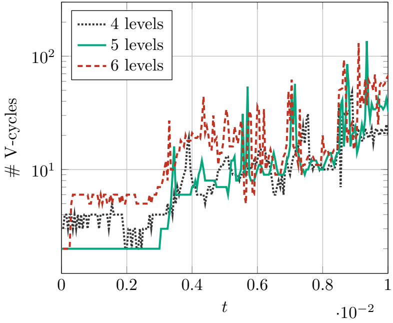

RMTR method

Number of nonlinear iterations/V-cycles as a function of time. Experiment performed for shear test.

Comparing computational time

Example	Stag. scheme	Monolithic scheme				
		TR		RMTR		
	time	time	reduction(Stag.)	time	reduction(Stag.)	reduction(TR)
Tension	9.06	6.41	29.24%	4.18	53.86%	34.79%
Shear	137.72	52.40	61.95%	21.32	84.52%	59.31%
Tear	123.15	48.16	60.89%	15.09	87.75%	68.67%

Execution time of simulations for three fracture modes ($782,340$ dofs). The time is measured in hours. Experiment performed in serial.

Computational complexity - RMTR method

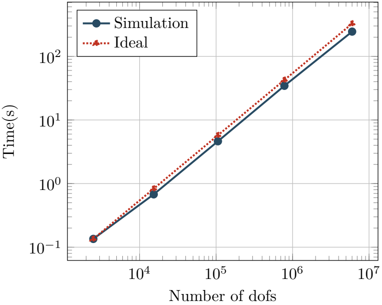

Computational complexity of the RMTR method. Experiment performed for tension test with 6 million dofs.

Large-scale fracture simulation

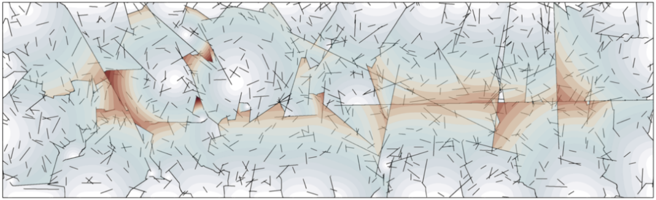

- Targets CPU-based computing architectures
- Implementation as part of library Utopia[Zulian, Kopanicakova et al. '17]
- Highly optimized (MPI, SIMD) FE assembly of phase-field fracture models
- Generation of stochastic fracture networks in 2D and 3D
- Scalable mutlilevel trust-region algorithm (RMTR)[Kopanicakova, Krause '20]

Zulian*, Patrick and Kopaničáková*, Alena and Nestola, Maria and Fink, Andreas and Fadel, Nur and VandeVondele, Joost and Krause, Rolf "Large scale simulation of pressure induced phase-field fracture propagation using Utopia" CCF Transactions on High Performance Computing. (2021)

Strong and weak scaling study

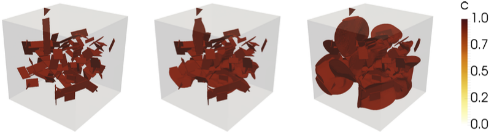

Strong scaling

fixed size: 122,657,188 dofs

RMTR with 4 levels

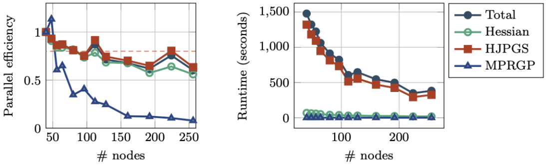

Weak scaling

size: 1,098,500 - 188,183,524 dofs

RMTR with 4 levels

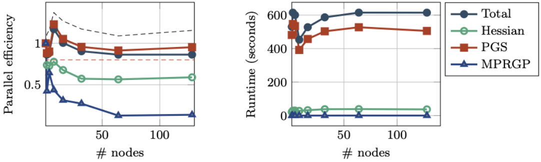

Experiment performed at CSCS, Piz Daint supercomputer, XC40 nodes (2 x 18 cores, 64/128 GB RAM). For weak scaling, the parallel efficiency $e = \frac{T_b}{T_n}$, where T_b is time of base experiment, while T_n is runtime on n nodes. For strong scaling, $e = \frac{T_b n_b}{T_n n}$, where n, n_b denotes number of nodes and nodes of base

Conclusion

- Additive and multiplicative Schwarz preconditioned inexact Newton's method for monolithic phase-field fracture systems
  - Decomposition performed using the field-split approach
- Numerical results demonstrate improvement in the performance compared to the standard AM method
  - The largest reduction of computational cost obtained for the problems with the gradual crack propagation
  - The speedup grows with increasing loading increments and the mesh resolution
- Globally convergent nonlinear multilevel method
  - Globalization performed by means of trust region strategy
  - Solution dependent objective functions are employed on every level
- Numerical results suggest very good performance of the RMTR algorithm
  - Compared to staggered scheme and single level TR method
  - RMTR method is of optimal complexity and scales well

References

Publications (selected):

- Kopaničáková A., Kothari H., Krause R. (2022) Nonlinear Field-Split Preconditioners for Solving Monolithic Phase-field Models of Brittle Fracture. Under review in Computer Methods in Applied Mechanics and Engineering
- Kopaničáková A., Krause R. (2020) A recursive multilevel trust region method with application to fully monolithic phase-field models of brittle fracture, Computer Methods in Applied Mechanics and Engineering, 360 (1)
- Zulian*, P., Kopaničáková*, A., Nestola, M.G.C. et al. (2021) Large scale simulation of pressure induced phase-field fracture propagation using Utopia. CCF Trans. HPC 3, 407–426
- Bilgen, C., Kopaničáková, A., Krause, R. et al. (2018) A phase-field approach to conchoidal fracture. Meccanica 53, 1203–1219.

Software:

- Frac SPIN: Implementation of Phase-field fracture and SPIN method
`https://bitbucket.org/alena_kopanicakova/pf_frac_spin`
- Utopia: A C++ embedded domain specific language for scientific computing
`https://bitbucket.org/zulianp/utopia`
- Moonolith: A library for parallel L^2 projections
`https://bitbucket.org/zulianp/par_moonolith`

International Multigrid Conference (IMG) in Lugano
August 22-27, 2022 (img2022.usi.ch)

Thank you for your attention.